small methods
www.small-methods.com

Relaxation Times of Ionic Liquids under Electrochemical Conditions Probed by Friction Force Microscopy

Florian Hausen

Ionic liquids (ILs) represent an important class of liquids considered for a broad range of applications such as lubrication, catalysis, or as electrolytes in batteries. It is well-known that in the case of charged surfaces, ILs form a pronounced layer structure that can be easily triggered by an externally applied electrode potential. Information about the time required to form a stable interface under varying electrode potentials is of utmost importance in many applications. For the first time, probing of relaxation times of ILs by friction force microscopy is demonstrated. The friction force is extremely sensitive to even subtle changes in the interfacial configuration of ILs. Various relaxation processes with different time scales are observed. A significant difference dependent on the direction of switching the applied potential, i.e., from a more cation-rich to a more anion-rich interface or vice versa, is found. Furthermore, variations in height immediately after the potential step and the presence of trace amounts of water are discussed as well.

1. Introduction

Ionic liquids (ILs) are room-temperature molten salts and represent an interesting class of liquids due to their remarkable properties, i.e., being nonvolatile and nonflammable.[1] These liquids have been considered for various applications ranging from solvent chemistry and catalysis,[2] to fuel cell,[3,4] and energy storage and conversion.[5,6] Especially in electrochemical applications, e.g., as electrolytes or electrolyte additives, the high reduction and oxidation stability of ILs and thus, their broad electrochemical window in combination with a high conductivity are of particular interest.[7] It has been shown in numerous experimental,[8–10] and theoretical,[11,12] publications that ILs form a distinct structure of cation and anion layers adjacent to electrified surfaces. These unique structures form an exponentially decaying force profile[13] and depend strongly on the exact potential applied to the electrode.[4,9–14] For many applications in which different potentials are applied at various times, e.g., in batteries during charging and discharging, supercapacitors or fuel cells information about the time required for reorganization of these layers to form a stable interface under alterable electrode potentials is of great importance.

Pioneering works in unraveling the relaxation times of ionic liquids as a function of applied potential have been utilizing current-based methods, such as electrochemical impedance spectroscopy (EIS). Based on EIS, Roling et al. reported a fast and slow process and analyzed the contribution of these processes to the overall differential capacitance.[15] Further studies have extended the methods to surface plasmon resonance (SPR) and X-ray reflectivity investigations (XRR). Nishi et al. demonstrated that there is an ultraslow relaxation in ILs by SPR and found variations depending of the direction of the potential step.[16] Reichert et al. identified three remarkably different relaxation processes of ionic liquids by EIS and XRR experiments.[17] The authors attributed those to cation and anion transport at time scales of a few milliseconds, to orientation and vertical rearrangements at times in the order of 100 ms and to lateral 2D-reorganization processes of the layers, taking part in the order of tens of seconds.

To investigate the interfacial structure of an IL adjacent to a charged surface, atomic force microscopy-based techniques are well-established, especially force–distance curves.[8,9,13,14,18] In addition, Black et al. investigated the 3D structure of ILs on a larger scale (100s of nm) based on force–distance curve mapping on a carbon surface.[19] Thereby, topological disordering is observed. Elbourne et al. resolved the 3D structure of ILs near a mica surface by amplitude-modulated AFM.[20] Endres et al. observed in electrochemical scanning tunneling microscopy (EC-STM) studies very slow changes of the surface and attribute this to slow reorientation processes of the ionic liquid.[21] Wen et al. reported video-EC-STM experiments, verifying the reorientation

F. Hausen
Forschungszentrum Jülich
Institute of Energy and Climate Research
IEK-9, 52425 Jülich, Germany
E-mail: f.hausen@fz-juelich.de

F. Hausen
RWTH Aachen University
Institute of Physical Chemistry
52074 Aachen, Germany

F. Hausen
INM-Leibniz Institute for New Materials
Campus D2 2, 66123 Saarbrücken, Germany

F. Hausen
Jülich-Aachen Research Alliance
Section: JARA-Energy
52425 Jülich, Germany

The ORCID identification number(s) for the author(s) of this article can be found under https://doi.org/10.1002/smtd.202300250

DOI: 10.1002/smtd.202300250

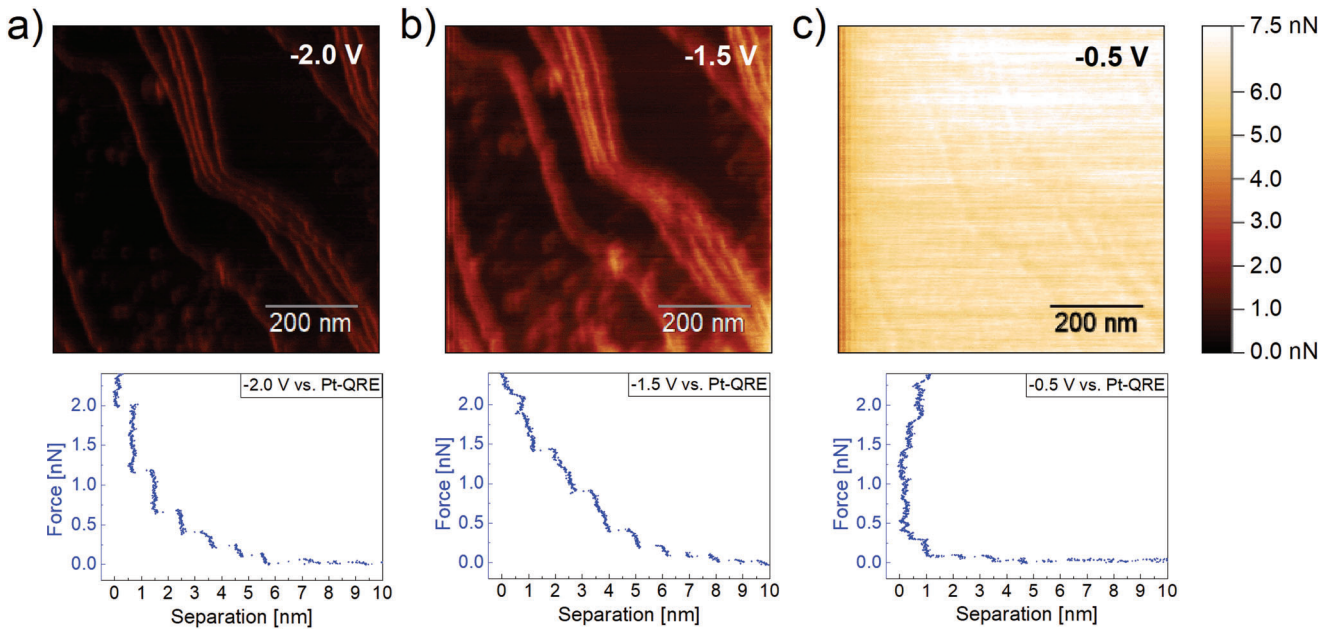

Figure 1. Friction force microscopy maps and force separation profiles of Au(111) in [$Py_{1,4}$]FAP at potentials of a) −2.0 V, b) −1.5 V, and c) −0.5 V versus Pt-QRE and single force–separation profiles under these conditions, respectively. The color represents the friction force with darker colors corresponding to lower values and brighter colors visualizing higher friction. The color scale is identical for all three images. The FFM maps are acquired with a normal load of 11 nN and a scanning speed of 6 Hz. The simultaneously recorded height images are provided in Figure S1 (Supporting Information).

processes of the ionic liquid interface as a function of potential and find rapid dynamic fluctuations at grain boundaries and defects.[22]

The aim of this study is to investigate the applicability of friction force microscopy (FFM), an atomic force microscopy-based technique, to study the relaxation times of ionic liquids in contact with electrified gold surfaces as long-term processes have been assigned to dynamic 2D lateral reorganization processes.[17] In FFM, the torsional response of the cantilever in contact with a surface is recorded. FFM in ionic liquids under electrochemical load has been pioneered by Sweeney et al. about a decade ago, demonstrating the extremely high sensitivity of friction forces to even subtle changes in the IL interface.[23] The progress since then has been excellently reviewed very recently.[24] Typically, variations in the friction value are induced by triangular variations of the potential with time, i.e., cyclic voltammetry or information are gathered at one fixed potential.

As typical electrochemical experiments can be performed in FFM, chronoamperometric experiments are also feasible. However, and despite the fact of its importance for many applications, none of the above-mentioned work addresses the relaxation times of ionic liquids when varying the sign of the applied potential. While the cation and anion transport processes are too fast to be analyzed with common FFM technique, the relaxation times of the orientational and lateral 2D-reorganization processes are in a reasonable range to be probed by FFM. Within this work, FFM as an imaging technique sensitive to lateral ordering is utilized for the first time to investigate the relaxation time of an ionic liquid. The hydrophobic ionic liquid, namely, 1-butyl-1-methylpyrrolidinium tris(pentafluoroethyl) trifluorophosphate ([$Py_{1,4}$]FAP) on Au(111) is probed as a well-characterized model system. Force–separation profiles and the frictional behavior,[13,14,23] as well as relaxation time investigations,[15,17] are published using this ionic liquid on various substrates. In this work, the relaxation times observed by FFM are compared with those from the current response during the chronoamperometric experiments. In addition, the influence of the switching direction of the potential, variations in height upon switching, and the effect of trace amounts of water are discussed.

2. Results and Discussion

2.1. Characterization of the Frictional Sensitivity on the Ionic Liquid Interfacial Structure

To ensure that the interfacial structure of the ionic liquid adjacent to the electrified Au substrate is not influenced by variations of the electrode's structure, experiments are conducted on atomically smooth single-crystalline gold surfaces. **Figure 1** shows FFM results for relatively large scans of 700 × 700 nm^2 at three different potentials. Variations in the color correspond to different friction values between the AFM tip and the ionic liquid layers on the gold, with brighter colors corresponding to higher friction values (Please note that the color scale for all three images is identical). Clearly, individual monoatomic steps, separating smooth terraces of about 200 nm, and several small islands are visible on the Au surface. The occurrence of islands is based on the lifting of the reconstruction of the Au(111) crystal. In addition, typical force–separation profiles for three applied potentials between −2 and −0.5 V are shown. Pronounced layering is found for −2 and −1.5 V with more than eight layers. At −0.5 V especially the layers adjacent to the surface undergo variations. Although several distinct layers are identified, the forces to push through those are

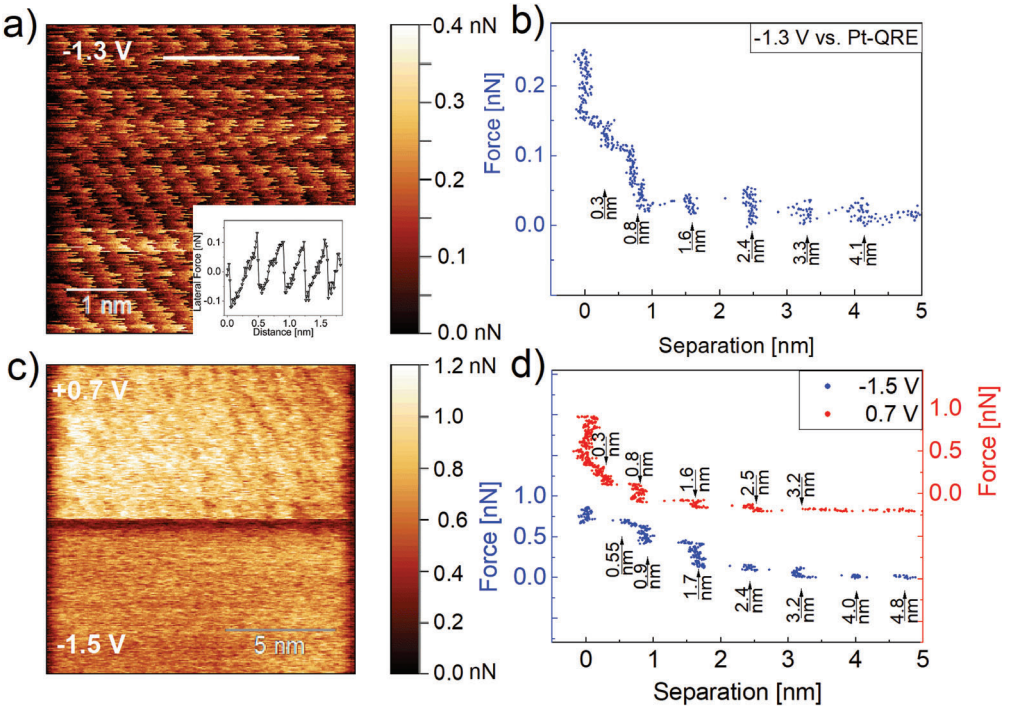

Figure 2. a) High-resolution FFM map at −1.3 V and a normal load of 1 nN, revealing a periodicity of 0.3 nm. The inset shows a typical stick-slip pattern as commonly observed for crystalline materials, and b) the respective force–separation profile. c) FFM map of the situations at −1.5 and +0.7 V, recorded with an applied normal load of 2.3 nN. d) Force–separation profiles at the respective applied potentials. Both profiles were recorded at the identical sample position. The curve at +0.7 V has been recorded with a waiting time of 2 min after the potential step. The corresponding height images for (a) and (c) are provided in Figure S2 (Supporting Information).

substantially reduced compared to the more negative potentials. In addition, for applied potentials of −1.5 and −0.5 V, the observed layers appear nonvertical. This effect is regularly reported in literature and attributed to a decrease in stiffness of the layers as a function of distance from the charged substrate.[4,9,14] This reflects a slightly compressible structure and is often observed for intermediate charged surfaces, such as mica,[9] or less strong applied potentials.[4,14]

In contrast to the severe variation of the friction force as a function of potential, indicated by the change in color, the underlying Au surface structure remains unchanged throughout the experiment and exhibits the same features in all FFM maps. Importantly, it is concluded that variations in the applied electrode potential have no significant impact on the Au substrate within the stability window of the ionic liquid. In addition, the presence of significant amounts of water is excluded as this would strongly influence the number of observed layers of the ionic liquid.[25,26] Therefore, by using single-crystal surfaces and focusing FFM maps on atomically smooth terraces, the interfacial structure is well resolved.

2.2. Determination of the Charge State of the Gold Surface at −1.5 and +0.7 V versus Pt-QRE

It is important to understand the charging state of the Au substrate for the potentials applied in the relaxation time measurements. **Figure 2**a shows a high-resolution FFM map of 3.8 × 3.8 nm^2 at an applied electrode potential of −1.3 V. A clear atomic lattice corrugation is detected, exhibiting a typical stick-slip pattern for atomic-scale FFM as shown in the inset. High-resolution maps of ionic liquids adsorbed on charged surfaces have been reported in literature. Elbourne et al. reported high-resolution images of the innermost and first-near surface interfacial layers of five different ionic liquids on negatively charged mica.[20] The authors reveal ordered structures, however, not comparable with high-resolution images of solid crystalline surfaces. Ebeling et al. also report high-resolution images of the IL propylammonium nitrate on HOPG.[27] However, the reported images have been obtained in dynamic AFM modes, whereas in this work FFM has been employed, in which the direct interaction between the AFM tip and the ionic liquid layers are much higher. Hence, it is unlikely that the obtained structure is representing the IL. An alternative explanation to the possibility that the periodicity is caused by a strongly adsorbed IL layer is, that the AFM tip at this potential might penetrate all layers down to the gold substrate. The obtained periodicity of about 0.3 nm is also reminiscent of what has been reported for Au(111) in an aqueous electrolyte.[28] This argument might be further supported by the force–separation profile depicted in Figure 2b. Two layers of 0.5 and 0.3 nm thickness are found at small separations. Hayes et al. studied the same system and report dimensions of 0.35 nm for the cation and 0.5 nm for the anion.[14] Those values are very close to the observed 0.3 and 0.5 nm layer shown in Figure 2b at an applied potential of −1.3 V. Although the low forces needed to push through indicate that there could be additional layers,[9] separated anion and

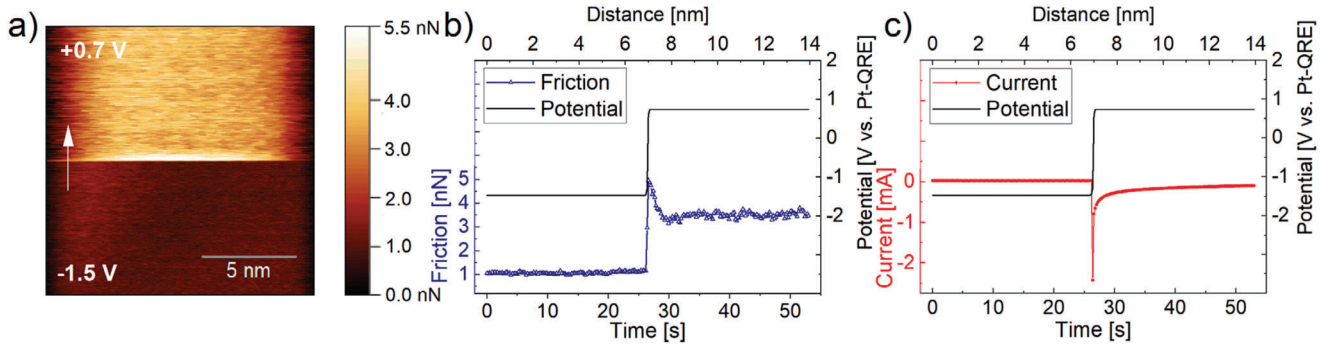

Figure 3. a) FFM map during the potential switch from −1.5 V (lower part) to +0.7 V (upper part) at a normal load of 9.7 nN and a scanning speed of 4.8 Hz. The color corresponds to the friction force and reveals a higher friction at +0.7 V compared to −1.5 V. Note the short drastic increase in friction immediately after the potential step at about half of the image. b) The extracted friction information from (a) as well as the corresponding applied potential as a function of scan distance or time. c) The simultaneously recorded temporal evolution of the current. The corresponding voltage and height maps are provided in Figure S3 (Supporting Information).

cation dimensions are typically not observed for layers at larger separations.[8,9,13,14] In agreement with these observations, the steps at larger separation in the force-separation curve shown in Figure 2b are about 0.8 nm apart, closely corresponding to the dimension of an ion pair of 0.9 nm.[14]

The situation changes when more negative or more positive potentials are applied as shown in Figure 2c: In the upper half of the 14 × 14 nm^2 image a potential of +0.7 V is applied to the electrode and an amorphous structure with increased friction (brighter color) is seen. At an applied potential of −1.5 V as recorded in the lower half of the image, the surface structure changes significantly, exhibiting a smoother appearance with less clusters, but overall lower friction. Both structures are separated by some scan lines exhibiting a strongly decreased friction (darker color).

The obtained force–separation profiles for these potentials are illustrated in Figure 2d. The overall appearance resembles earlier investigations on the interfacial structure of ionic liquids by AFM.[8,9,14] Importantly, a variation at small separations from the gold electrode is revealed for applied potentials of −1.5 and +0.7 V. As the dimension of these layers do not fit to the ion pair size, it is concluded that this layer is composed of anions or cations, depending on the potential, and that these inner layers cannot be penetrated by the AFM tip. This agrees with many force curves of various systems and is extensively documented in literature.[9,10,13,14] The friction force map and the force–separation curves shown in Figure 2c,d also illustrate the strong correlation between the interfacial structure of ionic liquids and the obtained friction. While recording the individual friction values for different numbers of layers is difficult in AFM, such an experiment was performed by a surface force balance.[29] The authors find individual friction values directly depending on the number of layers between the tribopair. A discussion about variations in height upon switching the potential is provided in Section 2.4. However, for this study it is important to verify the different charging of the Au surface, concomitant with a reorientation of the IL structure upon switching of the potential. The relaxation behavior of the IL under these conditions is analyzed in more detail from FFM maps as shown in Figure 2c and simultaneously recorded current profiles in the following Section 2.3.

2.3. Relaxation Behavior of [Py$_{1,4}$]FAP on Au(111) as Revealed by FFM

In this section, the relaxation process of the IL is investigated in more detail and as a function of normal load. As earlier work already reported a strong anisotropic behavior depending on the direction of the applied potential step, the results of this work are separately presented and then discussed jointly.[16] The FFM maps are 14 × 14 nm^2 in size to ensure homogeneous conditions with respect to roughness and interfacial layers.

In **Figure 3**, FFM maps and extracted profiles for the step from an applied electrode potential of −1.5 to +0.7 V is exemplarily shown for a normal load of 9.7 nN. The FFM map is characterized by an intermediate high friction signal (bright color), as depicted in Figure 3a. This is analyzed in more detail by plotting the frictional data as a function of distance and thus, as a function of time, as shown in Figure 3b. In addition, the respective voltage is shown. The simultaneously recorded temporal evolvement of the current is provided in Figure 3c.

The friction exhibits a low value of 1 nN at an applied normal load of 9.7 nN in the lower part of the image presented in Figure 3a, corresponding to the first ≈25 s of the image. Immediately with the change in the applied potential the friction is significantly increased and stabilizes after a short peak at a value of ≈3.5 nN after some seconds. At the same time the current that is recorded from the entire Au surface in contact with the IL exhibits the expected exponential decay based on capacitive currents. As indicated in **Figure 4** the relaxation time of the friction force is defined as the time until the friction has been stabilized after the potential jump. In the case of a capacitive current the exponential curve is fitted according to the formula

$$y = A \cdot e^{\frac{-x}{\tau_c}} \quad (1)$$

From an electrochemical perspective this corresponds to an RC circuit problem and is derived from the general equation for the charge on a capacitor as a function of potential.[30] Since the current decay has been found to be rather slow after this potential step, the current and friction (cf. Figure 4a) recorded in the subsequent FFM image was added to the data to obtain a reasonable

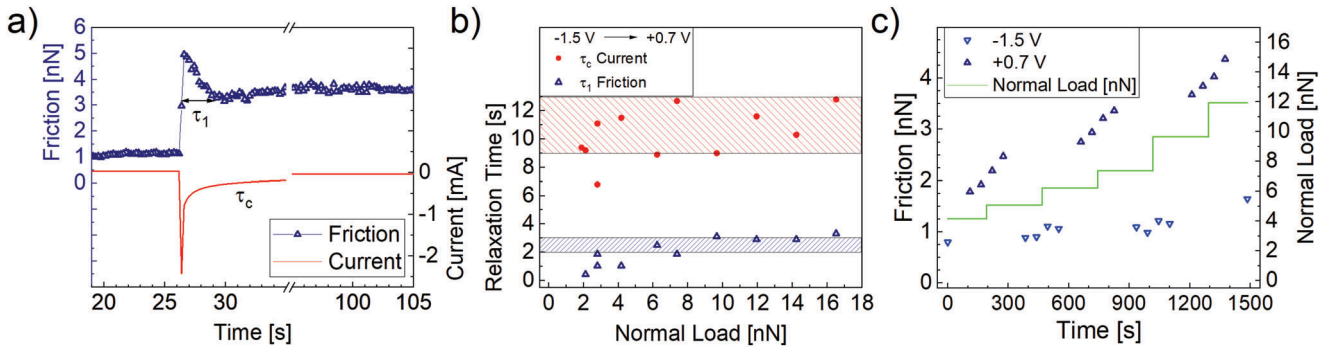

Figure 4. a) Definition of τ_1 and τ_c for the potential step from −1.5 to +0.7 V. b) Graphical visualization of τ_c and τ_1 for various normal loads. Note: The electrochemical data are recorded from the entire Au surface, while friction data represents the local situation. The shaded areas are meant as guides to the eye. c) Subsequent FFM data for −1.5 V and +0.7 V as a function of normal load. Each data point is the average of the inner part of a FFM frame of 14 × 14 nm^2, recorded with a scanning speed of 4.8 Hz. The applied potential is switched between upward and downward facing triangles, i.e., after four consecutive scans. The normal load is increased after four consecutive scans, two at each potential.

fit. The same experiment as shown in Figure 3 was conducted and analyzed for normal loads between 1.9 and 16.5 nN. Qualitatively, similar results are found for all normal loads applied and the results are provided in Table S1 (Supporting Information) and Figure 4b.

The initial drastic increase in friction is not related to the relaxation time of the current decay as observed in the chronoamperometric data and visualized in Figure 4b. Note that the electrochemical information is recorded from the entire Au surface in contact with IL, whereas the friction data are obtained from a small area of 14 × 14 nm^2 to avoid topographical contributions. Information about the relaxation times is gathered by extracting profiles as illustrated in Figure 4a. The origin of τ_c is the capacitive current flowing to account for the reorientation of the ionic liquid adjacent to the electrode. Roling et al. found a fast capacitive process in the order of 0.5 ms that cannot be detected by FFM.[15] In addition, the authors describe a slower capacitive process based on charge redistributions within the IL layers adjacent to the electrode that occurs in the range of seconds. While the relaxation time τ_c is found to be rather long with about 10 s in this work, the friction seems to be stabilized much faster after ≈2–3 s. However, due to the slow relaxation of the current response to the potential step, the subsequently recorded FFM maps are analyzed in detail as well and shown in Figure 4c. Each data point corresponds to a full FFM map of 14 × 14 nm^2 and upward facing triangles correspond to friction at +0.7 V. Between two images, the normal load has been increased as shown in green. Focusing on the friction at +0.7 V, it is found that each subsequent FFM map exhibits higher friction values than the maps before. In addition, the effect of the normal load increase is seen. However, this illustrates that friction is not stabilized after τ_1, but increases linearly with time over very long periods. Even in the fourth consecutive FFM map, recorded more than 5 min after the potential step, the friction has not reached a steady state.

In comparison, the situation is more complex after a potential step from +0.7 to −1.5 V as shown by the downward facing triangles in Figure 4c. For normal loads below 6 nN the subsequent FFM map exhibits a very similar friction than the previous map. The increase after two data points is due to the increase of normal load, accompanied with a higher friction value as reported earlier.[23] Albeit less clearly than for the potential step to +0.7 V, for loads higher than 6 nN the subsequent FFM map for the potential step to −1.5 V also show a reduced friction in subsequent images, indicating that the steady state is not reached. A more detailed view on the potential step from +0.7 to −1.5 V is shown in **Figure 5**. Similar to the results presented before, friction undergoes a strong change immediately after the potential step, indicated by the darker appearance in Figure 5a. However, in contrast to the former experiment, friction decays exponentially. A more detailed view on the temporal evolvement of the friction in Figure 4c reveals that the initial decaying process is much faster than in the case of the potential step from −1.5 to +0.7 V.

Figure 5c shows the simultaneously recorded current response to the potential step, exhibiting a typical exponential decay as expected as discussed earlier. τ_c is calculated by fitting the obtained current signal by Equation (1). τ_1 represents the time until the friction starts to decay exponentially as indicated in **Figure 6**a. The exact values obtained for all applied normal loads are provided in Table S2 (Supporting Information). As the electrochemical data are obtained from the entire crystal surface in contact with the IL, and as it cannot be influenced by the normal load, a constant value τ_c is expected, as depicted in Figure 6b. The less scatter compared to the values summarized in Table S1 (Supporting Information) and shown in Figure 4b is caused by better fits to the exponential decay for this potential step from +0.7 to −1.5 V. Interestingly, the relaxation time τ_c is with 2–3 s much shorter in this case, indicating that the reorganization of a more cationic layer adjacent to the charged Au(111) surface is faster than the respective anionic layer. This effect might be attributed to the size of the ions as the cations are significantly smaller than the bulkier anions. The relaxation time τ_1 is comparable to the values obtained for the potential step from - 1.5 V to 0.7 V. In contrast, the observed exponential decay of the friction with a relaxation time of τ_2, obtained by an exponential fit according to Equation (1) of the friction force is less expected. Although Smith et al. demonstrated by using a surface force balance (SFB) that friction can differ for one applied normal load if the number of layers between the tribopair vary,[29] only a stepwise change in friction would be reasonable. Hence, intralayer reorientation of IL ions

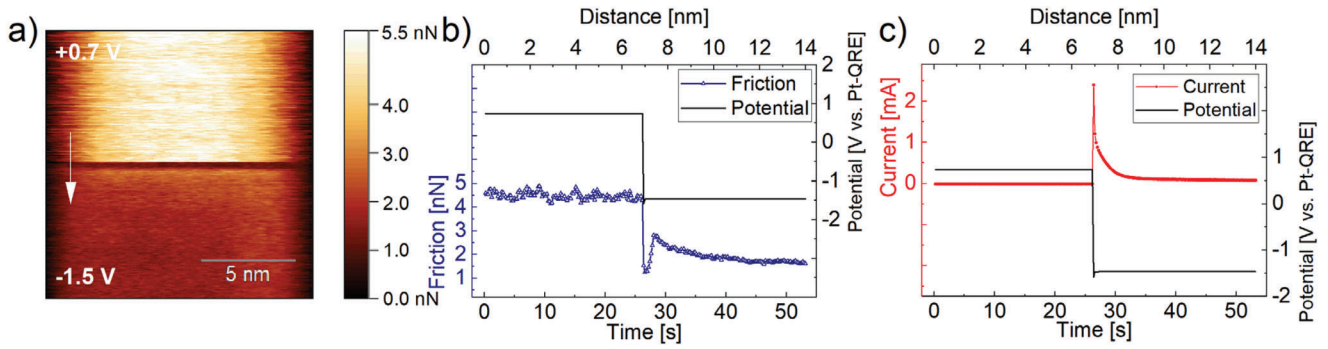

Figure 5. a) FFM map during the potential switch from +0.7 V (upper part) to −1.5 V (lower part) at a normal load of 11.9 nN and a scanning speed of 4.8 Hz. The color corresponds to the friction force and reveals a higher friction at +0.7 V compared to −1.5 V as already seen in Figure 4c. Note the short drastic decrease in friction immediately after the potential step at about half of the image. b) The extracted friction information from the center of (a) as well as the corresponding applied potential as a function of scan distance or time. c) The simultaneously recorded temporal evolution of the current.

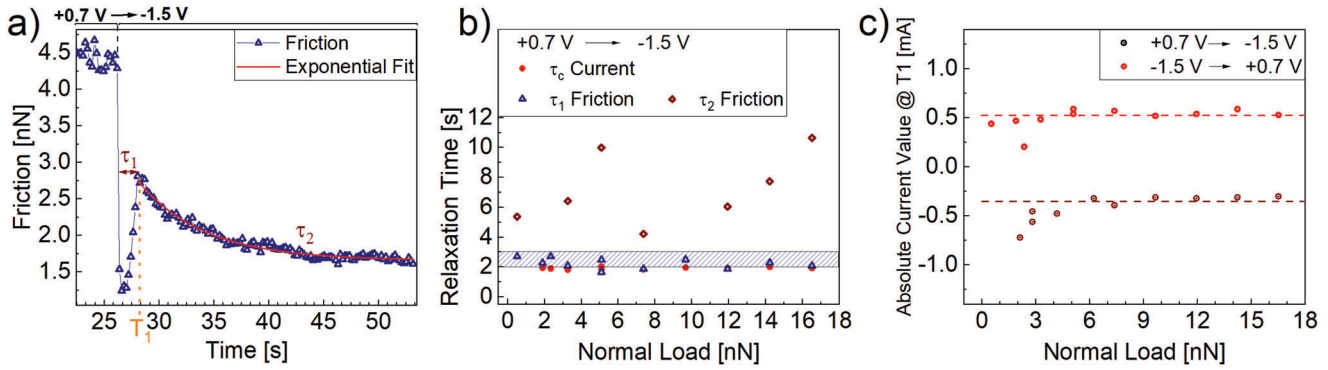

Figure 6. a) Definition of T_1, τ_1, and τ_2 for the potential step from +0.7 to −1.5 V. b) Graphical visualization of τ_1, τ_2, and τ_c. Note: The electrochemical data are recorded from the entire Au surface, while friction data represent the local situation. c) Absolute current value at T_1, as defined in (a).

are more reasonable to explain the observed trend. Interlayer ion exchange on the other hand is a slower process and might be accountable for the slower relaxation process.[16] Obtained values for τ_2 as shown in Figure 6b and summarized in Table S2 (Supporting Information) and are rather scattering. Such an effect was also discussed by Reichert et al. who attributed it to ion–electrode interactions and reorganization of substrate-adsorbed cations.[17] Both aspects would clearly induce heterogeneities that may cause variations in the local glide plane.[19] The broad distribution of τ_2 might be attributed to such effects. However, variations in the distance between the AFM tip and the electrode immediately after the potential step as it will be discussed in Section 2.4 makes a substrate-related interaction less likely compared to changes in the intralayer structural rearrangement.

An interesting observation is illustrated in Figure 6c: when analyzing the absolute current value at T_1, i.e., after τ_1 as defined in Figure 6a, a constant value for all measurements, despite variations in the normal load, is found for each direction of the potential step. This indicates that the electronic and frictional processes are related to each other. It is assumed that at this stage the rather quick inner layer reorientation is completed, and a constant surface charge is established. This might also be the reason why the τ_1 values are very similar, independent of the direction of the potential step.

2.4. Variation of Height during the Potential Steps

During the recording of the FFM maps as depicted in Figures 3a and 5a, the height of the tip is simultaneously recorded. The respective images are provided in Figures S3 and S4 (Supporting Information). **Figure 7** illustrates the result: for the different potential steps, different variations in height, i.e., the number of IL layers between the tip and surface, are observed as a function of normal load.

For the potential step from −1.5 to 0.7 V as depicted in Figures 3 and 4, no change in the height and thus, in the number of layers between scanning tip and Au surface, is observed, except for small variations of about 0.5 nm at the highest applied normal loads. In contrary, for the potential step from +0.7 to −1.5 V as illustrated in Figures 5 and 6, severe changes up to 2 nm are found for intermediate and high normal loads. This clearly shows that the obtained data for this step relates to different number of layers. Importantly, such an effect would have severe consequences for applications of ILs as lubricants in systems with different potentials. FFM experiments in ILs that are performed during continuous changes of the potential are only capable to measure relative changes in height and it remains undetermined if the tip indeed scans on the innermost IL layer directly adjacent to the charged surface or not. Typically, a change

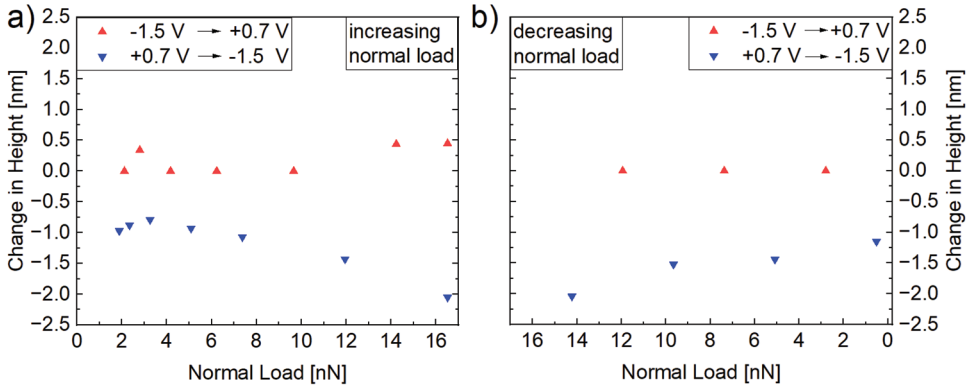

Figure 7. Variation in the height channel of the FFM upon changing the applied potential as a function of normal load. a) For increasing normal loads, b) while decreasing the normal load. For the potential step from −1.5 to +0.7 V almost no change in height is found, except for the highest applied normal loads, whereas the height is significantly affected by a potential step from +0.7 to −1.5 V. The information of each data point has been extracted from the height images recorded simultaneously with the data and provided in Figures S3 and S4 (Supporting Information), as well as in Tables S1 and S2 (Supporting Information).

in friction as a function of potential at the same normal load is explained by structural motives, such as different lubricating properties of anion and cations of the IL.[23,31] The observation made here could add an alternative explanation that the number of layers between the tribopairs are changing with the applied potential even if the normal load is not varied.[29] To answer this question, experiments with absolute distance control, like in SFB, should be performed. However, the change in height might be a result of electrostatic interactions between the tip and the change of the net charge at the Au surface.[32] Since the tip is made of highly doped silicon to avoid a charge accumulation such an effect is unlikely to occur in highly conductive ILs. The situation is expected to change when insulating cantilevers are used.

2.5. Relaxation Behavior of a Hydrophilic IL

Trace amounts of water are known to alter the dynamics and interfacial structure of ionic liquids adjacent to charged surfaces strongly, as demonstrated experimentally,[26,33,34] and by molecular dynamics simulations.[25] Fayer reviewed the dynamics and structure of various ILs and with respect to the water content.[35] To proof the hypothesis that the slow relaxation time τ_2 and the even slower relaxation observed after a potential step to positive voltages (cf. Figure 4c) is related to the individual interfacial structure of the ionic liquid, an experiment in 1-etyhl-3-methylimidazolium trifluoromethanesulfonate, [EMIm][OTf], containing about 200 ppm H_2O was conducted. The applied potentials of −1.5 and +1.5 V have been determined based on the obtained frictogram, i.e., the joint representation of electrochemical cyclic voltammetry and local friction data, as illustrated in **Figure 8**a. The CV is reminiscent of that for an Au(111) crystal in aqueous environment, exhibiting oxidation peaks and a clear reduction peak. At +1.5 V friction is clearly increased in the oxidative regime. In contrast, at −0.5 V the surface is expected to be reduced and the friction is low.

Figure 8b illustrates the slow relaxation behavior of the friction in the hydrophilic IL by subsequent recording of individual FFM maps in analogy to Figure 4c, where the same experiment for $[Py_{1,4}]FAP$ is shown. In stark contrast to the hydrophobic IL, the friction in [EMIm][OTf] stabilizes within one FFM image. As expected from typical FFM experiments friction increases when the normal load is raised.[23] Figure 8c shows that at −0.5 V the Au(111) substrate is resolved by FFM, in agreement with a less rigid interfacial structure as illustrated in Figure 8d. Hence, a clear influence of the rigidity of the interfacial structure on the slow relaxation time is considered likely. Furthermore, the clear deviations between the hydrophobic and hydrophilic ionic liquid illustrate the heterogeneous behavior of different ILs.

3. Conclusion

In summary, the relaxation time of a hydrophobic ionic liquid, namely, $[Py_{1,4}]FAP$, has been investigated by combined electrochemical and friction force microscopy experiments for the first time. Two different relaxation times, τ_1 and τ_2, are observed with respect to the friction force. τ_1 is rather independent of the direction of the potential step between −1.5 and +0.7 V or vice versa and in the order of 2–3 s, as shown in Figures 4b and 6b. τ_2 on the other hand strongly depends on the direction of the potential step. For the step from −1.5 to +0.7 V, a slight increase is indicated in Figure 4a; however, from Figure 4c it is verified that even after minutes no steady state has been reached. In contrast, for the step from +0.7 to −1.5 V, Figure 6a shows a clear exponential decay of the friction force after T_1 with relaxation times of τ_2 between 6 and 10 s. Thus, an anisotropic response of the lateral forces upon switching the potential is found in agreement with earlier reports.[16] The striking dependence of the observed friction behavior on the direction of the potential step is assigned to differences in the interfacial layer structure as a function of potential. Figure 2d verifies clear variations and a more robust and pronounced structure at −1.5 V compared to +0.7 V.

The faster relaxation process τ_1 is assigned to inner layer reorganization processes, while intralayer structural rearrangements of IL ions are responsible for the slower relaxation time τ_2. The latter is more severe for the potential step from +0.7 to −1.5 V as unveiled by the variations in height and extended τ_2 times. This

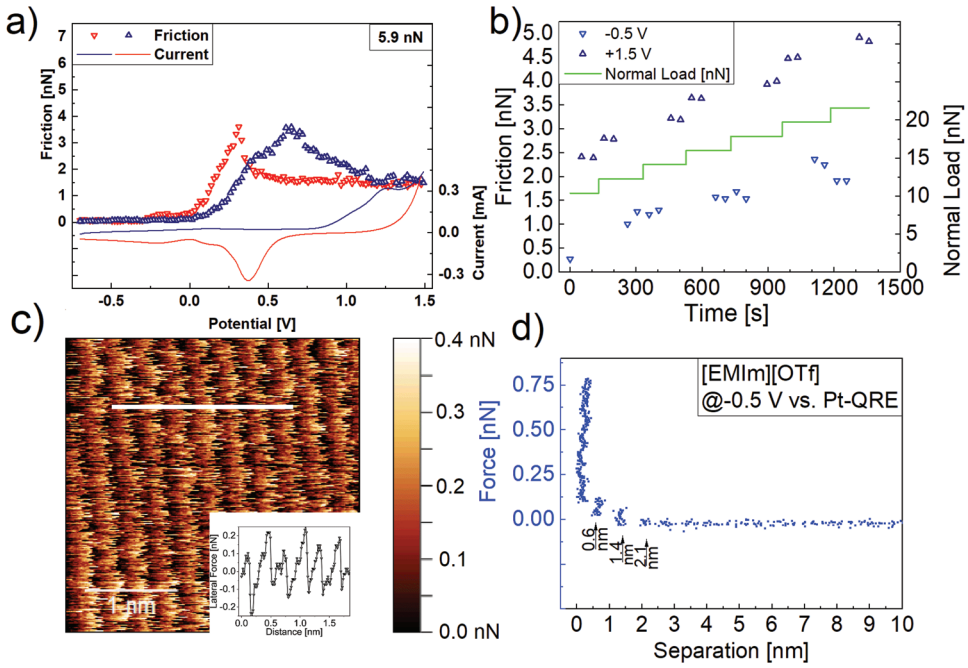

Figure 8. a) Frictogram, i.e., the joint representation of electrochemical cyclic voltammetry and friction data, for [EMIm][OTf] at a normal load of 5.9 nN and a scan speed of 6 Hz, revealing a strong dependence of friction on the applied electrode potential. b) Subsequent FFM data for [EMIm][OTf] on Au(111) at −0.5 and +1.5 V as a function of normal load. Each data point is the average of the inner part of a FFM frame of 7 × 7 nm^2, recorded with 42 nm s^{-1}. After four consecutive FFM maps, two for each applied potential, the normal load has been increased. The graph resembles that in Figure 4c, where the behavior of the hydrophilic IL is shown. c) High-resolution lateral force map of the Au(111) substrate at −0.5 V, revealing a crystalline atomic corrugation. Inset: stick-slip behavior at the position indicated by the white line. The corresponding height image is provided in Figure S5 (Supporting Information). d) Force–separation profile exhibiting a reduced number of interfacial layers and low forces to penetrate through.

is further supported as a more pronounced interfacial structure is obtained at −1.5 V as illustrated in Figure 2d.

FFM represents a new technique for precise measurements of relaxation times in ionic liquids that are related to lateral reorganization as well as vertical rearrangement. This research opens a better understanding of variations in ionic liquid interface structure und relaxation as a function of applied potentials and has important implications in energy storage, catalysis, and fuel cells if ILs are employed as electrolytes. Future work should include studies of various ILs of different viscosity[35] and with different amounts of water. Especially the relaxation times probed by FFM for the strong structural transition from monolayer to bilayers of interest.[36] In addition, more potential ranges and variations of the substrate should be investigated.

4. Experimental Section

The hydrophobic ionic liquid [$Py_{1,4}$]FAP (custom ultrapure synthesis by Merck, Germany, all impurities below 10 ppm) was received from the Endres group, Technical University of Clausthal, Germany, and was measured on an Au(111) substrate (Mateck, Germany). The hydrophilic ionic liquid [EMIm][OTf] was received from IoLiTec (Heilbronn, Germany) in 99.5% quality. Before each experiment, the Au(111) crystal was prepared by annealing in a butane flame for 1 min and cooling to room temperature for ≈2 h. All measurements were performed at room temperature. The setup also comprises a home-built electrochemical cell. Friction data were recorded by an Agilent 5500 AFM with built-in potentiostat. Cantilevers with sharp tips with a tip radius of curvature below 10 nm and a nominal normal spring constant of 0.2 N m^{-1} were used (PPP-Cont, Nanosensors) and individually calibrated for normal and torsional spring constants following the Sader method.[37] Each image contains 256 × 256 data points. Each data point shown in Figures 3b, 4a, 5b, and 6a was calculated as an average of 128 data points from each scan line from the inner part of the FFM map. Counter and reference electrodes were made of platinum wires. All potentials throughout the manuscript were quoted versus Pt-Quasi-reference electrode. To enhance the frictional sensitivity, the feedback gains were set to very low values. Friction was calculated as the difference between the lateral deflection of the cantilever in trace and retrace direction divided by two.[28] To avoid errors based on the turning of the cantilever, only the inner part of the FFM maps was used. Exceptions are the FFM maps shown in Figures 1, 2a, and 8c. To not lose the high resolution of the step edges or the substrate by a slight drift between trace and retrace scan, the mean value of a single retrace scan line was subtracted from each data point in trace direction in these cases. Force–distance curves received by the AFM contain must be converted to force–separation profiles for a direct reading of the distances by subtracting the compliance of the cantilever. This was done according to a procedure described by Senden.[38]

Supporting Information

Supporting Information is available from the Wiley Online Library or from the author.

Acknowledgements

The author is grateful to Roland Bennewitz, Rüdiger-A. Eichel, and L. G. J. de Haart for continuous support and fruitful discussion. The Endres group at the Technical University of Clausthal, Germany, is gratefully acknowledged for providing the ultrapure ionic liquid used in this study. The data

were recorded at the INM-Leibniz Institute of New Materials, Saarbrücken, Germany.

Open access funding enabled and organized by Projekt DEAL.

Conflict of Interest

The authors declare no conflict of interest.

Data Availability Statement

The data that support the findings of this study are available from the corresponding author upon reasonable request.

Keywords

friction force microscopy, ionic liquids, relaxation times

Received: February 26, 2023
Revised: July 14, 2023
Published online: August 7, 2023

[1] D. R. MacFarlane, M. Kar, J. M. Pringle, *Fundamentals of Ionic Liquids: From Chemistry to Applications*, Wiley-VCH, Weinheim, Germany **2017**.
[2] Z. Zhang, J. Song, B. Han, *Chem. Rev.* **2017**, *117*, 6834.
[3] M. Ebrahimi, W. Kujawski, K. Fatyeyeva, J. Kujawa, *Int. J. Mol. Sci.* **2021**, *22*, 5430.
[4] C. Rodenbucher, Y. Chen, K. Wippermann, P. M. Kowalski, M. Giesen, D. Mayer, F. Hausen, C. Korte, *Int. J. Mol. Sci.* **2021**, *22*, 12653.
[5] D. R. MacFarlane, N. Tachikawa, M. Forsyth, J. M. Pringle, P. C. Howlett, G. D. Elliott, J. H. Davis, M. Watanabe, P. Simon, C. A. Angell, *Energy Environ. Sci.* **2014**, *7*, 232.
[6] T. Stettner, A. Balducci, *Energy Storage Mater.* **2021**, *40*, 402.
[7] G. A. O. Tiago, I. A. S. Matias, A. P. C. Ribeiro, L. M. D. R. S. Martins, *Molecules* **2020**, *25*, 5812.
[8] R. An, A. Laaksonen, M. Wu, Y. Zhu, F. U. Shah, X. Lu, X. Ji, *Nanoscale* **2022**, *14*, 11098.
[9] J. M. Black, M. Zhu, P. Zhang, R. R. Unocic, D. Guo, M. B. Okatan, S. Dai, P. T. Cummings, S. V. Kalinin, G. Feng, N. Balke, *Sci. Rep.* **2016**, *6*, 32389.
[10] S. Perkin, *Phys. Chem. Chem. Phys.* **2012**, *14*, 5052.
[11] S. W. Coles, A. M. Smith, M. V. Fedorov, F. Hausen, S. Perkin, *Faraday Discuss.* **2018**, *206*, 427.
[12] A. A. Kornyshev, *J. Phys. Chem. B* **2007**, *111*, 5545.
[13] J. Hoth, F. Hausen, M. H. Muser, R. Bennewitz, *J. Phys. Condens. Matter* **2014**, *26*, 284110.
[14] R. Hayes, N. Borisenko, M. K. Tam, P. C. Howlett, F. Endres, R. Atkin, *J. Phys. Chem. C* **2011**, *115*, 6855.
[15] B. Roling, M. Druschler, B. Huber, *Faraday Discuss.* **2012**, *154*, 303.
[16] N. Nishi, Y. Hirano, T. Motokawa, T. Kakiuchi, *Phys. Chem. Chem. Phys.* **2013**, *15*, 11615.
[17] P. Reichert, K. S. Kjaer, T. Brandt van Driel, J. Mars, J. W. Ochsmann, D. Pontoni, M. Deutsch, M. M. Nielsen, M. Mezger, *Faraday Discuss.* **2017**, *206*, 141.
[18] G. Krämer, F. Hausen, R. Bennewitz, *Faraday Discuss.* **2017**, *199*, 299.
[19] J. M. Black, M. Baris Okatan, G. Feng, P. T. Cummings, S. V. Kalinin, N. Balke, *Nano Energy* **2015**, *15*, 737.
[20] A. Elbourne, K. Voitchovsky, G. G. Warr, R. Atkin, *Chem. Sci.* **2015**, *6*, 527.
[21] F. Endres, N. Borisenko, S. Z. El Abedin, R. Hayes, R. Atkin, *Faraday Discuss.* **2012**, *154*, 221.
[22] R. Wen, B. Rahn, O. M. Magnussen, *Angew. Chem., Int. Ed. Engl.* **2015**, *54*, 6062.
[23] J. Sweeney, F. Hausen, R. Hayes, G. B. Webber, F. Endres, M. W. Rutland, R. Bennewitz, R. Atkin, *Phys. Rev. Lett.* **2012**, *109*, 155502.
[24] F. Bresme, A. A. Kornyshev, S. Perkin, M. Urbakh, *Nat. Mater.* **2022**, *21*, 848.
[25] G. Feng, X. Jiang, R. Qiao, A. A. Kornyshev, *ACS Nano* **2014**, *8*, 11685.
[26] M. Han, R. M. Espinosa-Marzal, *ACS Appl. Mater. Interfaces* **2019**, *11*, 33465.
[27] D. Ebeling, S. Bradler, B. Roling, A. Schirmeisen, *J. Phys. Chem. C* **2016**, *120*, 11947.
[28] F. Hausen, N. N. Gosvami, R. Bennewitz, *Electrochim. Acta* **2011**, *56*, 10694.
[29] A. M. Smith, K. R. Lovelock, N. N. Gosvami, T. Welton, S. Perkin, *Phys. Chem. Chem. Phys.* **2013**, *15*, 15317.
[30] A. J. Bard, L. R. Faulkner, *Electochemical Methods: Fundamentals and Applications*, Wiley, New York **2001**.
[31] H. Li, M. W. Rutland, M. Watanabe, R. Atkin, *Faraday Discuss.* **2017**, *199*, 311.
[32] R. Bennewitz, M. Reichling, E. Matthias, *Surf. Sci.* **1997**, *387*, 69.
[33] H. W. Cheng, J. N. Dienemann, P. Stock, C. Merola, Y. J. Chen, M. Valtiner, *Sci. Rep.* **2016**, *6*, 30058.
[34] R. M. Espinosa-Marzal, A. Arcifa, A. Rossi, N. D. Spencer, *J. Phys. Chem. C* **2014**, *118*, 6491.
[35] M. D. Fayer, *Chem. Phys. Lett.* **2014**, *616*, 259.
[36] A. M. Smith, K. R. J. Lovelock, N. N. Gosvami, P. Licence, A. Dolan, T. Welton, S. Perkin, *J. Phys. Chem. Lett.* **2013**, *4*, 378.
[37] C. P. Green, H. Lioe, J. P. Cleveland, R. Proksch, P. Mulvaney, J. E. Sader, *Rev. Sci. Instrum.* **2004**, *75*, 1988.
[38] T. J. Senden, *Curr. Opin. Colloid Interface Sci.* **2001**, *6*, 95.

